Research article

Impact of superparamagnetic iron oxide nanoparticles (SPIONs) and ionic iron on physiology of summer squash (*Cucurbita pepo*): A comparative study

Huseyin Tombuloglu[a,*], Yassine Slimani[b], Guzin Tombuloglu[c], Ayse Demir Korkmaz[d], Abdulhadi Baykal[e], Munirah Almessiere[b,f], Ismail Ercan[b]

[a] Department of Genetics Research, Institute for Research and Medical Consultations (IRMC), Imam Abdulrahman Bin Faisal University, P.O. Box 34221, Dammam, Saudi Arabia
[b] Department of Biophysics, Institute for Research and Medical Consultations (IRMC), Imam Abdulrahman Bin Faisal University, P.O. Box 34221, Dammam, Saudi Arabia
[e] Department of Nanomedicine, Institute for Research and Medical Consultations (IRMC), Imam Abdulrahman Bin Faisal University, P.O. Box 34221, Dammam, Saudi Arabia
[c] Adnan Kahveci Mah., Mimar Sinan Cad., Mavisu evl., 7/28, Beylikduzu, Istanbul, Turkey
[d] Department of Chemistry, Istanbul Medeniyet University, 34700 Uskudar, Istanbul, Turkey
[f] Department of Physics, College of Science, Imam Abdulrahman Bin Faisal University, P.O. Box 1982, 31441 Dammam, Saudi Arabia

A B S T R A C T

This study investigates the effect of SPIONs (superparamagnetic iron oxide nanoparticles, ∼12.5 nm in size) on summer squash plant (*Cucurbita pepo*) in the presence and absence of supplementary iron (Fe(II)-EDTA). The plants were grown in nutrient solution with different iron sources: (i) Fe(II)-EDTA, (ii) without Fe(II)-EDTA (iii) SPIONs only, and (iv) Fe(II)-EDTA with SPIONs. Plant growth and development were assessed after 20 days of soaking by measuring phenological parameters such as plant biomass, chlorophyll content, amount of carotenoids, and the catalase enzyme activity. Transmission electron microscopy, inductively coupled plasma atomic emission spectroscopy, X-ray diffraction, and vibrating sample magnetometer methods were used to detect uptake and translocation of SPIONs in plant tissues. Our results showed that SPIONs treatment (without Fe(II)-EDTA) caused growth retardation and decreased the plant biomass and chlorophyll content. Hence, they are not efficient sources to compensate for iron demand of squash plant. Electron microscopy observations, magnetization and elemental analyses revealed that SPIONs are taken-up by plant roots but not translocate to upper organs. In roots, SPIONs use a symplastic route for intercellular transfer. These findings suggest that as an iron source, SPIONs alone are not efficient for plant growth, but can contribute it together with Fe(II)-EDTA.

1. Introduction

Nanoparticles (NPs), which are in the size range from 1 to 100 nm, have emerged in the last fifty years and are used in many practical applications including material science, electronics, medicine and pharmacology (Nikalje, 2015). Moreover, in the last decade, efforts to use NPs in agriculture such as nano-formulations for efficient fertilization, nanosensors for early detection of stressors, or nano-devices for effective genetic manipulations have increased tremendously (Prasad et al., 2014; Pérez-de-Luque, 2017). Iron-containing NPs (iron oxides) are one of the most popular materials, which have been proposed as potential fertilizer to treat iron deficient soil (Abadía et al., 2011; Rui et al., 2016). Low solubility of the iron (III) ion in the soil limits the iron uptake by plants and therefore the symptoms of iron deficiency occur in plants (Zuo and Zhang, 2011; Samaranayke et al., 2012). This situation can cause iron deficiency in animals and human through nutrition as well (White and Broadley, 2009).

In comparison to traditional iron fertilizers, Fe_2O_3 NPs enhanced the growth of peanuts, a plant which is very sensitive to iron deficiency (Rui et al., 2016). In addition, superparamagnetic iron oxide NPs (SPIONs, Fe_3O_4) treatment increased chlorophyll levels in soybean (Ghafariyan et al., 2013); and the mass of 1000-seeds (by 7%), the iron content (by 34%), and chlorophyll level (by 10%) in black-eyed peas (Delfani et al., 2014). In opposite to these findings, several studies have

showed that iron oxide NPs (magnetites) cause detrimental effects (Mushtaq, 2011; García et al., 2011; Marusenko et al., 2013; Barhoumi et al., 2015; Ma et al., 2013). Due to their potential phytotoxic and genotoxic effects on plants, ecologically responsible disposal of wastes containing those NPs is required (Aslani et al., 2014).

In addition to the indeterminate effects on plants, the bioaccumulation of these NPs in the plant body remains a challenge awaiting for further investigation (Fadeel et al., 2017). The possible accumulation of iron oxide NPs in plants as well as their transmission from plants to animals and/or humans is a matter of concern (Rai et al., 2018). For that reason, the uptake and translocation of NPs on plant body should be studied in lab scale before large-scale applications. So far, the translocation of Fe_3O_4 NPs from root to leaf has been shown in soybean (Ghafariyan et al., 2013), pumpkin (Zhu et al., 2008), and common bean (Govea-Alcaide et al., 2016). In opposite to these findings, Wang et al. (2011), Li et al. (2018), and Konate et al. (2018) reported that Fe_3O_4 NPs were unable to translocate in ryegrass, pumpkin, cucumber, and *Citrus maxima*.

These controversial results revealed the requirement of extensive investigations about the impact and translocation of iron oxide NPs on plants. Therefore, in this study, uptake and translocation of SPIONs were investigated on summer squash plant (*Cucurbita pepo*), one of the members of Cucurbitaceae. In addition, whether SPIONs were a potential source of iron for plants were evaluated by comparing them with the commonly used iron source, Fe(II)-EDTA. Comprehensive analyses were conducted on plant parts by using VSM, ICP-OES, XRD, and TEM analyses. In addition, physiological and enzymatic responses of the plant under iron deficient and single or combined iron containing conditions were assessed.

2. Material and methods

2.1. Characterization of SPIONs

The SPIONs were purchased from Sigma Aldrich. Phase identification and purity of SPIONs were analyzed using X-ray powder diffraction (XRD; Rigaku Benchtop Miniflex 600) with Cu Kα radiation. A TEM sample was prepared by depositing a droplet of SPIONs dispersed in ethanol onto the TEM grid. TEM was operated at accelerating voltage of 80 kV. The XRD powder pattern and TEM image of used SPIONs are given in Fig. 1a and b, respectively. All the observed diffraction peaks are indexed by the cubic structure of Fe_3O_4 (ICDD card no: 16–929). The mean size of the crystallites was estimated from the diffraction pattern by line profile fitting method using the Debye-Scherrer equation $D_{XRD} = \frac{0.9\,\lambda}{\beta\,cos\theta}$, where D_{XRD} is the average crystallites size, λ is the X-ray wavelength, β is the full width at half maximum (FWHM) and θ is the Bragg diffraction angle. The average crystallite size, D_{XRD}, was calculated to be about 12.5 nm. The TEM image indicates that the average particle size is about 13 nm, which is in accordance with XRD. Vibrating sample magnetometer (VSM) analysis was used to investigate the magnetic behavior of the SPIONs (Fig. 1c). It is obvious that SPIONs exhibits superparamagnetic behavior, with a saturation magnetization M_s ~60 emu/g in addition to negligible values of remanent magnetization (M_r) and coercive field (H_c).

2.2. Growth conditions and SPIONs exposure

Cucurbita pepo (summer squash) seeds (n = 15) were germinated in Petri plates for five days in dark. Uniform seedlings were transferred to Hoagland solution containing 6 mM KNO_3, 1 mM $NH_4H_2PO_4$, 2 mM $MgSO_4$, 4 mM $Ca(NO_3)_2$, 50 μM H_3BO_3, 9 μM $MnCl_2$, 0.3 μM $CuSO_4$, 0.8 μM $ZnSO_4$ and 0.12 μM MoO_3 (85%) (Hoagland and Arnon, 1950; Tombuloglu et al., 2013, 2015). The solution was modified by including or excluding Fe(II)-EDTA (25 μM, ~8.6 mg/L) and/or SPIONs (100 mg/ L) (Hu et al., 2017). Accordingly, nutrient solutions amended either

with (i) Fe(II)-EDTA only (= control, "Plant A″), (ii) without Fe(II)-EDTA or SPIONs ("Plant B″), (iii) SPIONs treatment alone without Fe (II)-EDTA ("Plant C″), and (iv) SPIONs with Fe(II)-EDTA ("Plant D″) were prepared. By doing so, plant growth settings mimicking both iron efficient and deficient environments were prepared. The solutions were sonicated for 30 min before application to minimize the agglomeration of SPIONs (Powersonic 410, Hwashin Technology, Korea) while the pH of the solutions was kept constant at 5.8. The seedlings were grown under greenhouse conditions (16:8 h light/dark cycle, 60–70% humidity, and 23–26 °C temperature) for three weeks. Meanwhile, the nutrient solution was aerated by an air pump (30 min every 3 h). Fresh and dry weight, tissue lengths, chlorophyll and carotenoids contents, soluble protein content, and catalase enzyme activities were measured after 20 days of the treatment.

2.3. Determination of soluble protein content and catalase activity

50 mg of fresh root and leaf samples were harvested from the plants and grounded in ceramic mortar filled with pre-cold 0.15 M phosphate buffer (pH 7.8) containing 1 mM EDTA. The extract was centrifuged for 20 min at 4 °C (15 000 × g). The aqueous phase was collected and used to determine the soluble protein content. Coomassie Brilliant Blue G-250 solution and BSA (bovine serum albumin) standards (6.25–200 mg/ L) were prepared and the absorbance of reaction mixture was measured by a spectrophotometer at 595 nm (Biotek, Synergy Neo2). The catalase enzyme activity was determined by using 10 μg of soluble protein according to previously described methods (Aebi, 1984; Tombuloglu et al., 2018). The consumption of H_2O_2 in every 30 s was recorded by reading the absorbance at 240 nm. The enzyme activity was calculated according to the following equation:

$$C\ (min-1.\ mg-1\ protein)\ =\ (Abs_0-Abs_1)\ /\ (\varepsilon\ .\ Cprot\ .\ t\ .\ d)\ .\ v$$

where, Abs_0 and Abs_1 are the absorbance value at 240 nm after 1 min interval. ε is the H_2O_2 extinction coefficient (39.4 M^{-1} cm^{-1}), d is size of cuvette path (cm), t is time between the measurement (min), C_{prot} is the amount of protein in the test tube (mg), v is volume of the test sample in cuvette (mL).

2.4. Measurement of chlorophyll and carotenoids

The content of chlorophyll *a, b*, and carotenoids were determined according to procedure by Lichtenthaler and Wellburn (1983). 50 mg of fresh leaf samples were cut into small pieces and mixed with 4 mL of %80 acetone. The homogenate was centrifuged at 4000 × g for 15 min. The absorbance (663, 646, and 470 nm) were measured from the collected supernatant by using a plate reader (Biotek, Synergy Neo2). The following equations were used to calculate the chlorophyll *a, and b*, and carotenoids contents, respectively:

$$Chl_a\ =\ 12.21 \times A_{663}\ -\ 2.81 \times A_{646}$$

$$Chl_b\ =\ 20.13 \times A_{646}\ -\ 5.03 \times A_{663}$$

$$Car\ =\ (1000 \times A_{470}\ -\ 3.27 \times Chl_a\ -\ 104 \times Chl_b)\ \div\ 227$$

2.5. Iron content analysis

0.5 g of root and leaf tissues were harvested from all tested plants. In order to clean the adsorbed NPs on the root surface, the roots were immersed in water and sonicated for 5 s (Powersonic 410, Hwashin Technology, Korea), and thoroughly washed with distilled water several times. The tissues were dried in an oven (60 °C) for three days and grounded in a mortar with a pestle. They were digested in a digiPrep hot block digestion system (SCP Science, Quebec, Canada) according to the United States Environmental Protection Agency (1996). Shortly, a (1:4) mixture of nitric acid (HNO_3, 65%) (SCP Science, Thermo Fisher), and hydrogen peroxide (H_2O_2, 30%) (Sigma-Aldrich) was poured on the
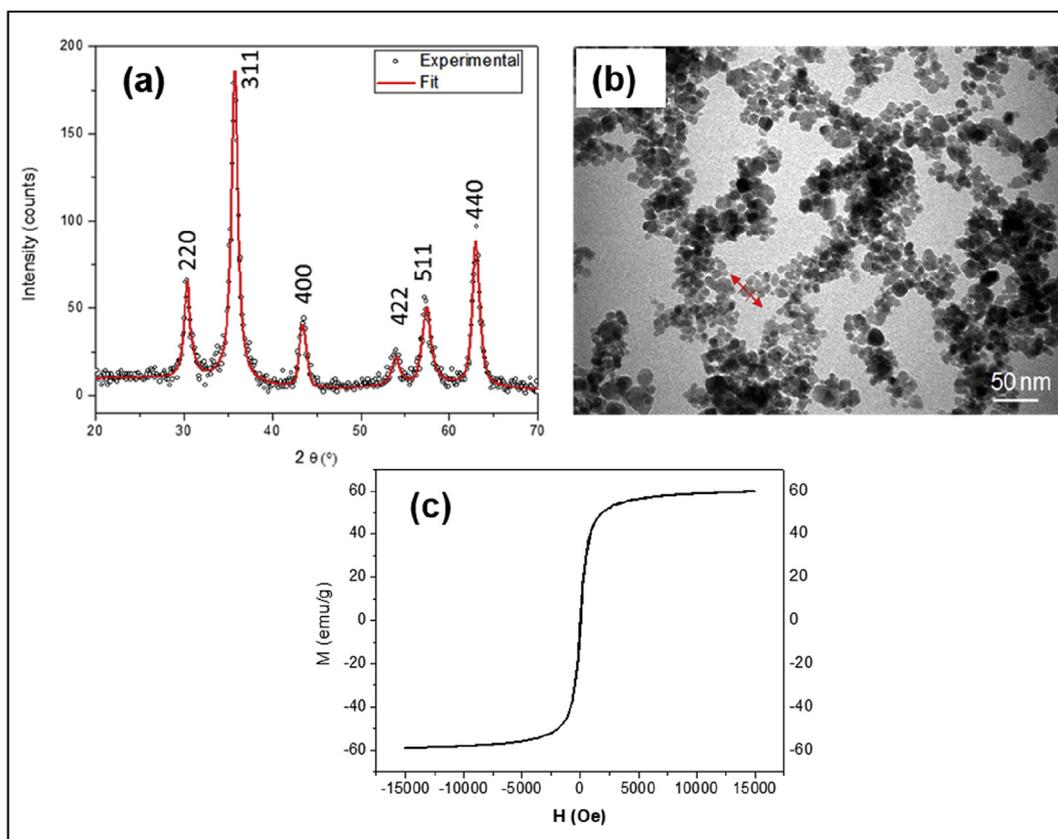
Fig. 1. (A) XRD powder pattern, **(b)** TEM image, and **(c)** magnetic behavior of SPIONs used during the growth of squash plant.
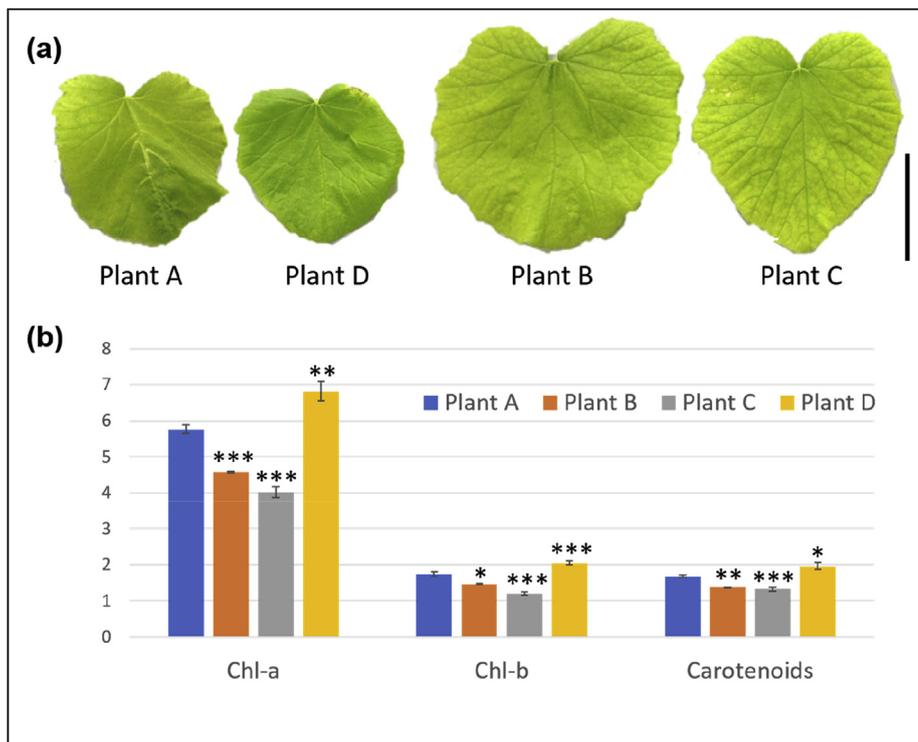

Fig. 2. Impact of SPIONs and Fe(II)-EDTA on plant growth and pigmentation **(a)** Images show the first true leaf after one week of the application (Scale bar, 5 cm). **(b)** Graph represents the pigment content (chlorophyll *a and b*, and carotenoids) of leaves after 20 days of soaking. The data was statistically analyzed by *t*-test (*p < 0.05, **p < 0.01, ***p < 0.005). Data are mean $\pm$ SE of three replicates. Plant A: Fe(II)-EDTA or control, Plant B: without Fe(II)-EDTA or SPIONs, Plant C: SPIONs alone, Plant D: SPIONs with Fe(II)-EDTA.

dry powder which was then heated up to 180 °C for 30 min. The iron (Fe) content was determined with an inductively coupled plasma optical emission spectroscopy (ICP-OES) (PerkinElmer AvioR 145 500 ICP-OES Scott/Cross-Flow, USA) instrument.

2.6. Ultrastructure analysis

Roots and leaves of summer squash plants treated with or without SPIONs (100 mg/L) were sampled after washing with PBS and placed in
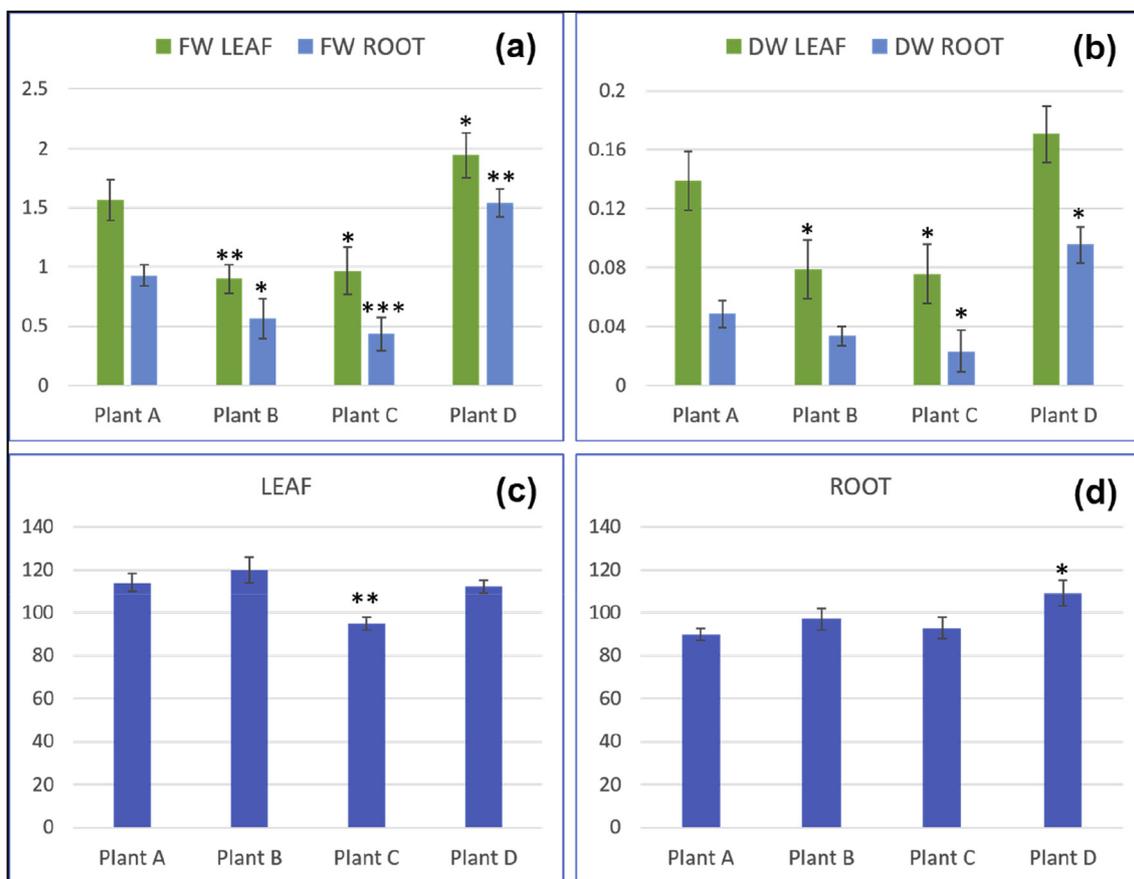
Fig. 3. Impact of iron sources on **(a)** fresh weight (FW) and **(b)** dry weight (DW) of squash plants. The values were represented in grams. **(c)** and **(d)** show the soluble protein content (μg/ml) of the leaf and the root samples, respectively. The data shows the mean ± SE of three replicates and was statistically analyzed by t-test (*$p < 0.05$, **$p < 0.01$, ***$p < 0.005$). Plant A: Fe(II)-EDTA or control, Plant B: without Fe(II)-EDTA or SPIONs, Plant C: SPIONs alone, Plant D: SPIONs with Fe (II)-EDTA.

an automatic tissue processor (Leica EM TP, Leica Microsystems, Belgium). The tissues were fixed in phosphate buffer (pH 7.2) including 3% glutaraldehyde and 1% osmium tetroxide (OsO_4) and, rinsed with 0.1 M PBS (pH 7.4) three times. Then, the tissues were dehydrated in a series of graded ethanol and acetone solutions in water increasing up to 100% concentration. Afterwards, the samples were embedded in epoxy resin and cured in an oven for 2 days at 60 °C. Ultrathin sections (75 nm) were cut on an ultra-microtome (Leica EM UC7, Leica Microsystems, Belgium) and stained with 2% uranyl acetate and 2% lead citrate. Subsequently, the sections were examined using a Morgagni™ 268 transmission electron microscope (TEM) (FEI, Eindhoven, The Netherlands).

2.7. Statistical analysis

All experiments were carried out with randomized sets including at least triplicate sampling. The data was statistically analyzed by t-test (*$p < 0.05$, **$p < 0.01$, ***$p < 0.005$). The values were presented as means ± SE (standard error) of at least three technical replicates. SPSS program version 15.0 (SPSS Inc., Chicago, USA) was used for statistical analyses.

3. Results

3.1. Effects of SPIONs on growth and pigment content

In Fig. 2a, the first true leaf of squash plants treated by different iron sources, either SPIONs or Fe(II)-EDTA, is displayed. The treatment of the plant with SPIONs and Fe(II)-EDTA supplementation (Plant D)

showed no visible morphological changes. However, the leaf color was darker than the control leaves (Plant A). As it was shown in Fig. 2b, it can be attributed to increased content of pigments (chlorophyll *a, b*, and carotenoids), which were significantly higher (~17%, $p < 0.01$; ~18%, $p < 0.005$; and ~16%, $p < 0.05$, respectively) in "Plant D" when compared to "Plant A". When compared to the control plant, the use of SPIONs as an iron source instead of Fe(II)-EDTA (Plant C) increased the leaf size, turned the leaf color to light green, and decreased the pigment content (chlorophyll *a, b*, and carotenoids) significantly similar to the results obtained from iron deficient plant (Plant B). These results show that SPIONs are not a good source of iron for squash plants.

3.2. Effects of SPIONs on plant biomass

The SPIONs treatment in the absence of Fe(II)-EDTA (Plant C) decreased the fresh weight (FW) and dry weight (DW) of the leaf and root tissues significantly (at least $p < 0.05$) (Fig. 3a and b). The decrease in FW was recorded as ~38% ($p < 0.05$) in leaves, and ~%53 ($p < 0.005$) in roots, compared to non-treated (control) plants. This result revealed that the applied dose of SPIONs is not enough to led the growth of squash plants as it was done by Fe(II)-EDTA in "Plant A", probably due to the inadequate iron content in the nutrient solution. On the other hand, the SPIONs treatment with Fe(II)-EDTA (Plant D) had an opposite effect where the plant biomass in root and leaves was significantly (at least $p < 0.05$) increased in comparison to the control (Plant A) plant. The enhancement was recorded for the FW by ~24% and ~66%; and for the DW by ~22% and ~96% in leaf and root tissues, respectively (Fig. 3a and b).
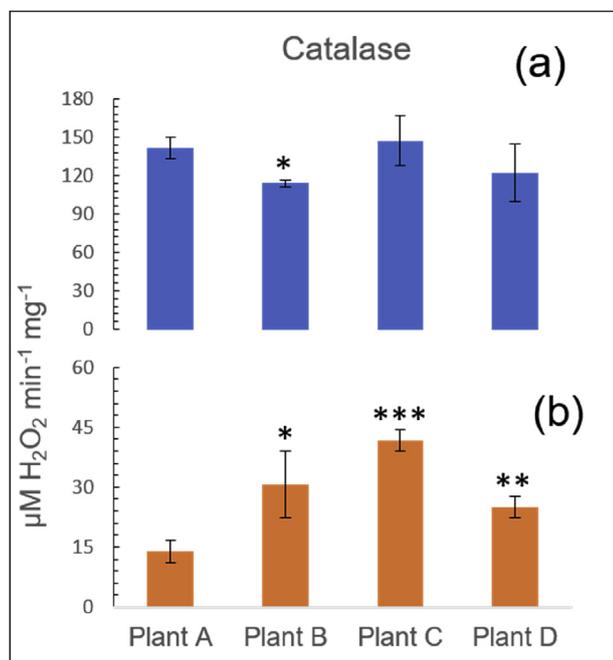
Fig. 4. Catalase activity in the leaf **(a)** and root **(b)** tissues from the plants subjected with or without different iron sources. The data was statistically analyzed by *t*-test (*$p < 0.05$, **$p < 0.01$, ***$p < 0.005$). Data are mean ± SE of three replicates. Plant A: Fe(II)-EDTA or control, Plant B: without Fe(II)-EDTA or SPIONs, Plant C: SPIONs alone, Plant D: SPIONs with Fe(II)-EDTA.

3.3. Impact of SPIONs on soluble protein content and catalase activity

Fig. 3c and 3d represent the soluble protein content of leaf and root specimens after being supplied by different iron resources, respectively. Compared to control group, the replacement of Fe(II)-EDTA with SPIONs (Plant C) decreased the soluble protein content in leaves significantly ($p < 0.01$, 16%). When SPIONs were added into the solution with Fe(II)-EDTA (Plant D), the root protein content was increased significantly ($p < 0.05$) by comparing to the control plant (Plant A).

Fig. 4 represents the activity of catalase enzyme. Among the leaf specimens, a significant reduction was observed in the plant with iron deficiency (Plant B) ($p < 0.05$). In contrast, the catalase activity in the roots increased significantly both in iron deficient (Plant B) and SPIONs-treated seedlings (Plant C and D) (at least $p < 0.05$).

3.4. XRD analysis

The XRD powder patterns of root and leaf samples of squash plant are presented in Fig. 5. When compared to the diffractogram of the control root plant (Plant A), some additional peaks were detected in the roots of plants "C" and "D". This confirms that the root organs absorb the SPIONs. However, these additional peaks between diffractograms in the various leaf samples of the squash plant do not exist. This reveals that the SPIONs are not transferred to the leaf tissues.

3.5. Microscopy analysis

Ultrastructure analysis of SPIONs-treated plants was carried out to observe the cellular uptake and the route of SPIONs in the plant body. In Fig. 6, the TEM analyses revealed that SPIONs (~12.5 nm in size) can penetrate the root cells (Fig. 6c and d). However, the presence of SPIONs was not observed in the leaf samples (Fig. 6a and b). In the roots, SPIONs are abundantly found at the periplasmic spaces and the cell wall structure. In addition, SPIONs were observed at plasmodesmata, channels that enable cell-to-cell connection and nutrient

transport (Fig. 6e and f).

3.6. Magnetization analyses

Analyses by a vibrating sample magnetometer (VSM) were conducted in order to confirm the uptake of SPIONs by squash plant. Fig. 7 presents the curves of magnetization against an applied magnetic field of ± 10 kOe, M(H), for various root specimens of squash plants; A (control), B (without Fe(II)-EDTA), C (SPIONs treatment alone without Fe(II)-EDTA) and D (applied dose of SPIONs with Fe(II)-EDTA). The M(H) analysis indicates that the root specimens of "Plant A" is a combination of paramagnetic (PM) and ferromagnetic (FM) behavior, where the PM dominates. The germination of squash plant in water free of Fe(II)-EDTA (Plant B) leads to decrease slightly the magnetization magnitude compared to the one of control plant. Furthermore, it is obvious that the root specimens of "Plant B" reflect practically a PM behavior. This is mostly due to the absence of Fe nutrient element in nutrient solution. In addition, the SPIONs treatment alone without Fe(II)-EDTA (Plant C) increases the magnetization magnitudes of root specimens. The M(H) curve of this sample showed a well-defined ferromagnetic nature with values of saturation magnetization (M_s), remanent magnetization (M_r), and coercive field (H_c) equal to 1.65 emu/g, 0.15 emu/g, and 300 Oe, respectively. The magnitude of magnetization shows a unique increase in root specimens of squash plants grown in the presence of Fe(II)-EDTA and SPIONs (Plant D) compared to other roots of squash plants. The root specimens of "Plant D" displays a superparamagnetic (SPM) behavior. For this sample, the value of M_s is equal to 9.1 emu/g. The M_r and H_c, with values equal respectively to 0.5 emu/g and 30 Oe, respectively, are negligible confirming the superparamagnetic behavior. The manifestation of the SPM nature is principally owing to the presence of SPIONs. This result confirms that the root specimens absorb noticeable amounts of SPIONs.

M(H) measurements were explored in root, stem and leaf tissues of "Plant A" and "Plant D" in order to evaluate the translocation of SPIONs to aerial organs. The M(H) plots are presented in Fig. 8. The applied dose of SPIONs ("Plant D") showed a SPM nature, confirming that noticeable amounts of SPIONs were absorbed by root organ. On the other hand, the M(H) hysteresis loops of stem and leaf of "Plant A" (controls) indicate a diamagnetic (DM) behavior in these specimens (Fig. 8c and e). This is contrarily different to that observed in the control root sample. It is clearly seen that the M(H) behavior changes suddenly in the stem of "Plant D" compared to the control one (Fig. 8d). Nevertheless, this magnetic behavior reveals the occurrence of a mixture of DM and SPM phases. However, the leaf of "Plant D" is less sensitive to the inclusion of SPIONs. The magnetization behavior indicates that there is a combination of DM and FM phases however, the DM phase dominates in this sample (Fig. 8f). The obtained findings reveal that the absorbed amounts of SPIONs by root organs are not translocate to the leaf organs.

3.7. Iron content in plant tissues

In order to confirm the uptake and migration of iron elements to the plant aerial organs, the iron content in root and leaf organs of all tested plants was determined (Table 1). As it is expected, iron deficient plants (Plant B) has the less iron content in its tissues. However, the plants supplemented with both SPIONs and Fe(II)-EDTA (Plant D) harbor the highest iron content (~250 mg kg^{-1} DW) in their roots. Compared to control plant (Plant A), it seems that the SPIONs addition contributed to the iron level of plants. The comparison of plant iron contents in "Plant C" (SPIONs only) and "A" (control, Fe(II)-EDTA only) shows that the applied dose of SPIONs (100 mg/L) is not sufficient to achieve the level of iron content obtained from control plants. Furthermore, the leaf iron content of "Plant C" (10.37 mg kg^{-1} DW) is almost the same as that of iron deficient plant, "Plant B" (8.47 mg kg^{-1} DW). These results point out that SPIONs are unable to translocate to the aerial organs of squash
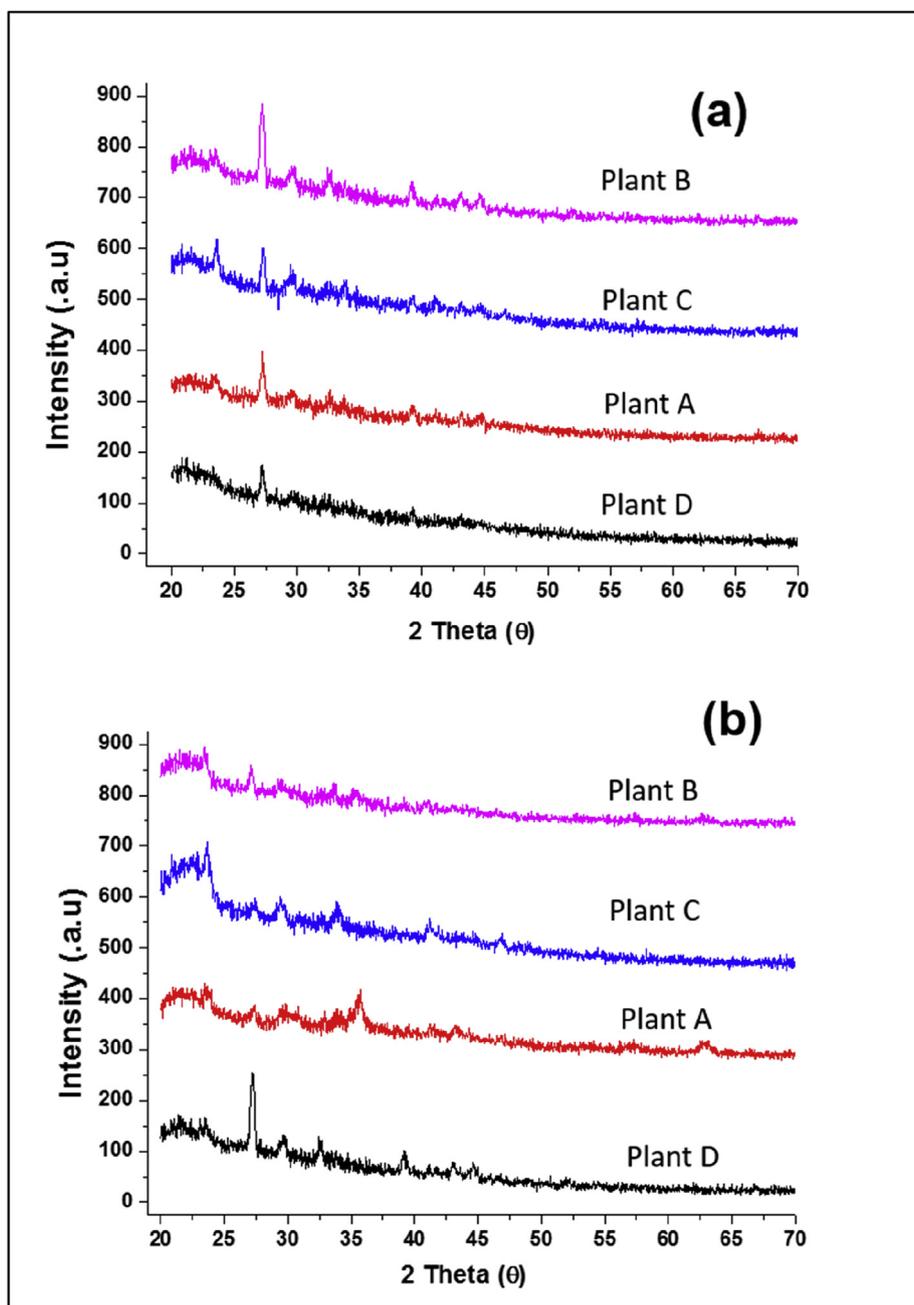
Fig. 5. XRD pattern of plant samples from **(a)** leaf and, **(b)** root. Plant A: Fe(II)-EDTA or control, Plant B: without Fe(II)-EDTA or SPIONs, Plant C: SPIONs alone, Plant D: SPIONs with Fe(II)-EDTA.

plant, which is displayed in Figs. 5 and 6.

4. Discussion

Nanoparticles have been successfully implemented in agriculture for the purposes of plant growth regulation and quality enhancement (Parisi et al., 2015). In addition, they are proposed to remediate plants suffering from nutrient deficiencies, such as iron (Rui et al., 2016), magnesium (Delfani et al., 2014), and calcium (Hua et al., 2015). Compared to traditional fertilizers, nano-fertilizers allows better dissolution and faster absorption and assimilation by the plant (Morales-Díaz et al., 2017). Therefore, they can enhance plant-growth in certain concentration ranges and be used in agricultural applications to increase agronomic yields of crops and/or minimize environmental pollution (Liu and Lal, 2015).

In this study, it was shown that the use of SPIONs as an iron source instead of Fe(II)-EDTA is not sufficient to compensate the iron demand of squash plants. In contrast, the treatment with SPIONs alone caused growth retardations and symptoms like iron-deficiency in plants (Fig. 2a). For instance, leaves of iron deficient plant (Plant B) were found to be yellowed and expanded. The increase in the leaf area is a kind of adaptation to enable efficient photosynthesis against low iron content (Fernández et al., 2008). Since the iron is required to produce chlorophyll and photosynthetic enzymes (Rout and Sahoo, 2015), the abundance of chlorophyll a, b, and carotenoids were decreased significantly ($\sim 20\%$, $p < 0.005$; $\sim 15\%$, $p < 0.05$; and $\sim 18\%$, $p < 0.01$, respectively) in the iron deficient plant (Plant B) when compared to the control plant (Plant A). Similar results were obtained for the plants grown in nutrient solution amended with SPIONs only (Plant C) (Fig. 2b). Furthermore, the plant biomass (FW and DW) were
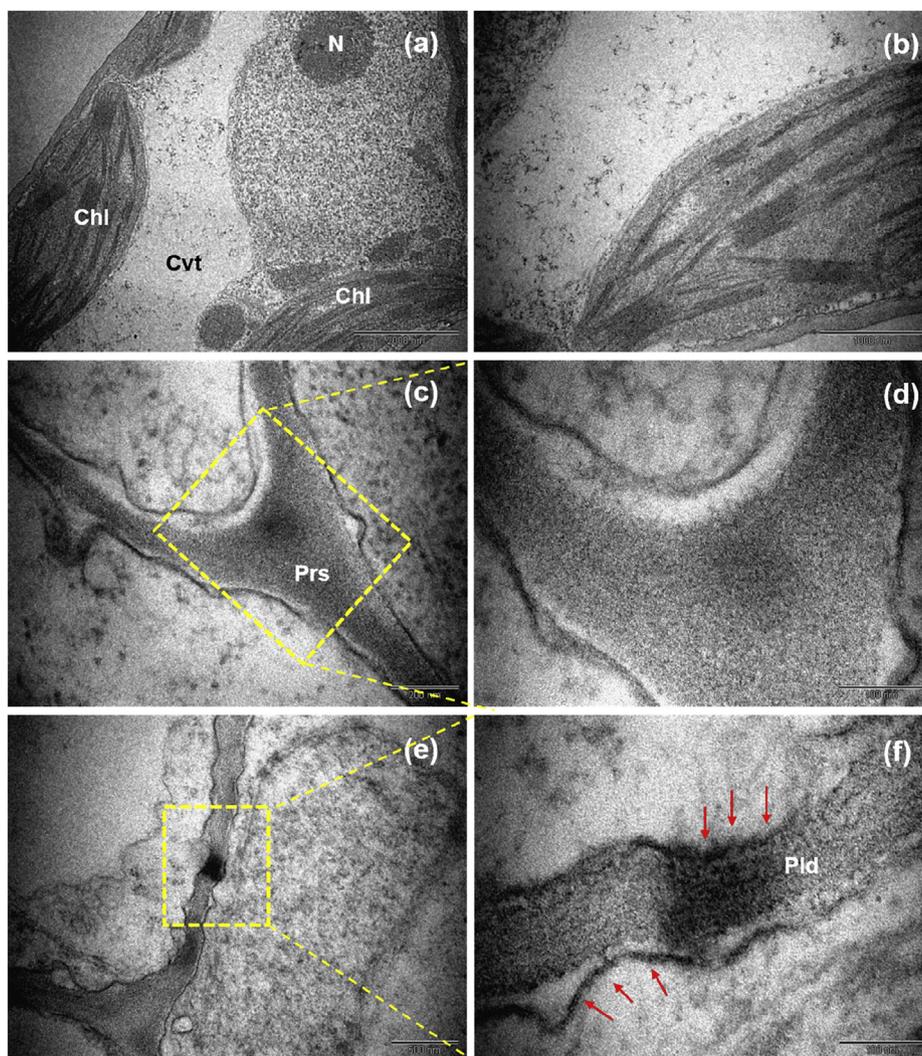
Fig. 6. TEM observation of (**a, b**) the leaf and (**c-f**) the root cells from SPIONs treated squash seedlings (Plant D). (**a, b**) No SPIONs were observed in the leaves. (**c, d**) It is obvious that SPIONs accumulated in the periplasmic space (Prs) and (**e, f**) attached to the cell wall (cw). In addition, they are abundant at plasmodesmata (Pld), cell to cell communication unit, suggesting a symplastic route for their cellular translocation. Chl: Chloroplast, N: nucleus, Cyt: cytoplasm.
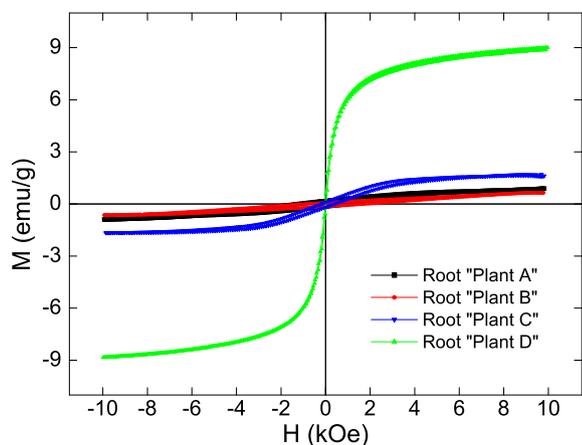

Fig. 7. M(H) curves of various root specimens of squash plants A, B, C and D. Plant A: Fe(II)-EDTA or control, Plant B: without Fe(II)-EDTA or SPIONs, Plant C: SPIONs alone, Plant D: SPIONs with Fe(II)-EDTA.

decreased which is in turn parallel to these findings (Fig. 3a and b). A possible explanation of the decreased growth could be that SPIONs are unable to serve as an iron source for the metabolic processes of the

plant completely. The disassociation of iron elements from iron oxide nanoparticles may partially contribute to the iron demand of plant as shown a previous study by Hu et al. (2017) in which a negligible amount of $Fe^{3+}14$ □) µg/L) is dissolved from γ-Fe_2O_3 NPs suspended in Hoagland solution.

The presence of SPIONs affected the protein content of the leaves and roots differently (Fig. 3c and d). The increase in the soluble protein content of roots could be attributed to the enhanced *de novo* synthesis of defensive or stress-related proteins for cell protection (Teixeira et al., 2005). On the other hand, the decrease in leaf protein content can be explained due to the reductions in the activity of some enzymes such as RuBisCo which depresses the synthesis of protein and accelerates their degradation thus creates an imbalance in soluble amino acid/protein ratio (Baroowa et al., 2016; Surendar et al., 2013). Similarly, the activity of the catalase enzyme was different in root and leaf tissues (Fig. 4). In roots, dramatic increases were obtained from all tested groups which is attributable to the production of reactive oxygen species (ROS). Previous studies have observed similar findings (Moore, 2006; Hund-Rinke and Simon, 2006). However, it is obvious that SPIONs-treatment did not alter the enzyme activity in leaves, probably due to the prevented transfer of SPIONs to the aerial organs.

The existence of SPIONs in the root cells were verified by TEM and XRD analyses. However, no SPIONs were found in the leaf parts (Figs. 5
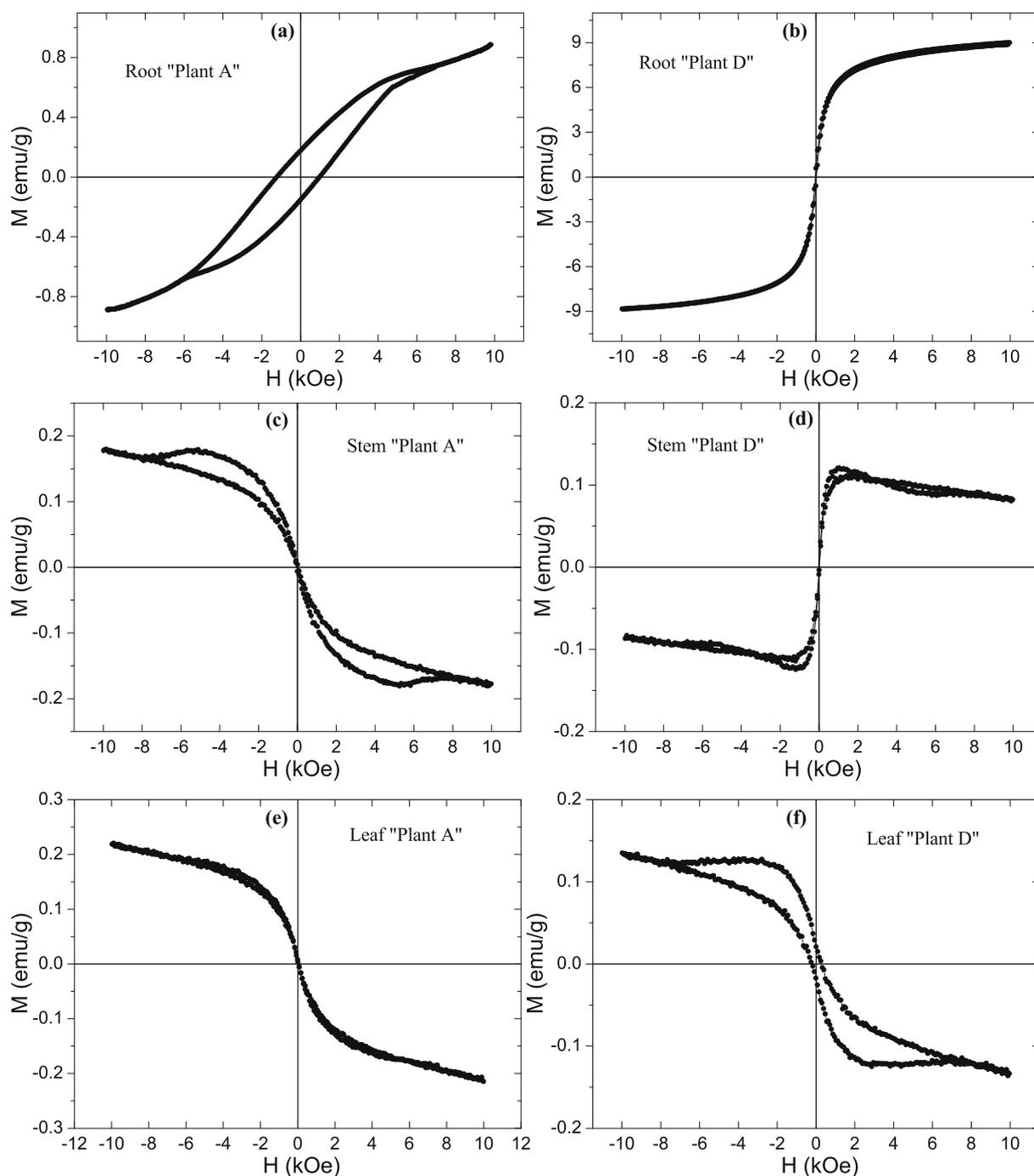
Fig. 8. M(H) curves of the different root, stem and leaf organs of squash "Plant A" (left) and "Plant D" (right). Plant A: Fe(II)-EDTA or control, Plant D: SPIONs with Fe(II)-EDTA.

Table 1
Iron (Fe) content of root and leaf tissues (mg kg^{-1} DW).

Samples	ROOT	LEAF
"Plant A"	196.33 ± 17.2	80.37 ± 10.1
"Plant B"	25.17 ± 8.1	8.47 ± 6.5
"Plant C"	100.06 ± 19.1	10.37 ± 4.6
"Plant D"	254.87 ± 8.4	43.70 ± 5.6

and 6). Nanoparticles can enter the plant cells and may be transported either apoplastically or symplastically from one cell to another via plasmodesmata (Rico et al., 2011; Zhai et al., 2014). In our study, SPIONs were abundantly found at this structure (plasmodesmata)

which serve as the channels enabling cell-to-cell communication and transport. This finding suggests that SPIONs use a symplastic transport route in pumpkin through plasmodesmata.

Since SPIONs have magnetic character, their involvement in plant parts was investigated by VSM analysis (Fig. 6). The data of M(H) are divided by the mass of the sample. Therefore, the magnetic signal strength is linked to the magnetic material concentration. This means that the greater the magnetic signal is, the greater the concentration of magnetic nanoparticles will be. It is obvious that the magnetic responses collected for the various root squash specimens are very smaller than the magnetization of SPIONs alone (~60 emu/g) (Fig. 1c), which is an expected result. This observation agreed with the previous investigations done by Tombuloglu et al. (2018).

Table 2
Studies representing the translocation of SPIONs in different plants.

NPs	Size	Plant	Translocation	Reference
Fe$_3$O$_4$	9 nm	Soybean	Yes	Ghafariyan et al. (2013)
	20 nm	Pumpkin	Yes	Zhu et al. (2008)
	~10 nm	Common bean	Yes	Govea-Alcaide et al. (2016)
	25 nm	Ryegrass, pumpkin	No	Wang et al. (2011)
	20 nm	*Citrus maxima*	No	Li et al. (2018)
	~6.7 nm	Cucumber	No	Konate et al. (2018)
	~12.5 nm	Squash	No	This study
γ-Fe$_2$O$_3$	~17.7 nm	Maize	No	Li et al. (2016)

Moreover, the iron content analysis by ICP-OES showed a negligible amount of iron is transferred to the leaves upon SPIONs treatment (Plant C) (Table 1). These findings are in agreement with previous studies. For instance, the uptake of SPIONs without being translocated to leaves has been shown in ryegrass, pumpkin (Wang et al., 2011), cucumber (Konate et al., 2018), and *Citrus maxima* (Li et al., 2018). On the other hands, their translocation has been shown in soybean, pumpkin, and common bean in some studies (Table 2). It is obvious that the translocation is dependent on the plant type. Despite the small size of NPs, different plants can have different "mechanisms" that ultimately affect NPs translocation. For example, biological structures, such as the cell wall, Casparian strip and the cell membrane with sizes ranging from 1 to 100 nm (depending on the plant species) can prevent or allow NPs to pass through cells or organs (Wang et al., 2016). In addition, the size of plant cell wall pores varies between 3.5 nm and 20 nm (Chichiricco and Poma, 2015). The size distribution of the SPIONs in this study is around 12.5 nm which would allow them to penetrate cells. However, due to the magnetic nature of SPIONs, they can form agglomerates in the plant body which in turn increases their size and hence may prevent their translocation.

5. Conclusion

In this study, the uptake and translocation of SPIONs (~12.5 nm in size) were investigated and their effects on summer squash were evaluated by comparing with ionic iron (Fe(II)-EDTA). The magnetization, XRD, and elemental analyses revealed that SPIONs were up-taken by roots but could not pass into leaf tissues, probably due to several size exclusion limits (i.e. cell wall, Casparian strip, or cell membrane). In the roots, SPIONs use a symplastic transport route through plasmodesmata. The treatment of the plant with SPIONs alone (without Fe(II)-EDTA) caused retardation in growth and biomass, therefore it can be concluded that SPIONs are not efficient sources to compensate for iron demand of the squash plant. Overall, these results suggest that as an iron source, SPIONs alone are not sufficient to meet the iron requirement of the plant. However, they can contribute to the iron concentration of the summer squash when used with Fe(II)-EDTA.

Author contribution

HT and GT carried out plant growth and physiological experiments. YS studied on magnetization and VSM analyses. AB and MA conducted on the nanoparticle characterization experiments. IE determined the iron content. ADK revised the manuscript.

Conflicts of interest

The authors declare no conflict of interest.

References

Abadía, J., Vázquez, S., Rellán-Álvarez, R., El-Jendoubi, H., Abadía, A., Álvarez-Fernández, A., López-Millán, A.F., 2011. Towards a knowledge-based correction of iron chlorosis. Plant Physiol. Biochem. 49 (5), 471–482.

Aebi, H., 1984. [13] Catalase in vitro. Methods in Enzymology, vol. 105. Academic Press, pp. 121–126.

Aslani, F., Bagheri, S., Muhd Julkapli, N., Juraimi, A.S., Hashemi, F.S.G., Baghdadi, A., 2014. Effects of engineered nanomaterials on plants growth: an overview. ScientificWorldJournal 2014.

Barhoumi, L., Oukarroum, A., Taher, L.B., Smiri, L.S., Abdelmelek, H., Dewez, D., 2015. Effects of superparamagnetic iron oxide nanoparticles on photosynthesis and growth of the aquatic plant Lemna gibba. Arch. Environ. Contam. Toxicol. 68 (3), 510–520.

Baroowa, B., Gogoi, N., Farooq, M., 2016. Changes in physiological, biochemical and antioxidant enzyme activities of green gram (Vigna radiata L.) genotypes under drought. Acta Physiol. Plant. 38 (9), 219.

Chichiricco, G., Poma, A., 2015. Penetration and toxicity of nanomaterials in higher plants. Nanomaterials 5 (2), 851–873.

Delfani, M., Baradarn Firouzabadi, M., Farrokhi, N., Makarian, H., 2014. Some physiological responses of black-eyed pea to iron and magnesium nanofertilizers. Commun. Soil Sci. Plant Anal. 45 (4), 530–540.

Fadeel, B., Pietroiusti, A., Shvedova, A.A. (Eds.), 2017. Adverse Effects of Engineered Nanomaterials: Exposure, Toxicology, and Impact on Human Health. Academic Press.

Fernández, V., Eichert, T., Del Río, V., López-Casado, G., Heredia-Guerrero, J.A., Abadía, A., et al., 2008. Leaf structural changes associated with iron deficiency chlorosis in field-grown pear and peach: physiological implications. Plant Soil 311 (1–2), 161.

García, A., Espinosa, R., Delgado, L., Casals, E., González, E., Puntes, V., et al., 2011. Acute toxicity of cerium oxide, titanium oxide and iron oxide nanoparticles using standardized tests. Desalination 269 (1–3), 136–141.

Ghafariyan, M.H., Malakouti, M.J., Dadpour, M.R., Stroeve, P., Mahmoudi, M., 2013. Effects of magnetite nanoparticles on soybean chlorophyll. Environ. Sci. Technol. 47 (18), 10645–10652.

Govea-Alcaide, E., Masunaga, S.H., De Souza, A., Fajardo-Rosabal, L., Effenberger, F.B., Rossi, L.M., Jardim, R.F., 2016. Tracking iron oxide nanoparticles in plant organs using magnetic measurements. J. Nanoparticle Res. 18 (10), 305.

Hoagland, D.R., Arnon, D.I., 1950. The water-culture method for growing plants without soil, 2nd edit. California agricultural experiment station, Circular, pp. 347.

Hu, J., Guo, H., Li, J., Wang, Y., Xiao, L., Xing, B., 2017. Interaction of γ-Fe$_2$O$_3$ nanoparticles with Citrus maxima leaves and the corresponding physiological effects via foliar application. J. Nanobiotechnol. 15 (1), 51.

Hua, K.H., Wang, H.C., Chung, R.S., Hsu, J.C., 2015. Calcium carbonate nanoparticles can enhance plant nutrition and insect pest tolerance. J. Pestic. Sci. 40 (4), 208–213.

Hund-Rinke, K., Simon, M., 2006. Ecotoxic effect of photocatalytic active nanoparticles TiO2 on algae and daphnids. Environ. Sci. Pollut. Res. 13 (4), 225–232.

Konate, A., Wang, Y., He, X., Adeel, M., Zhang, P., Ma, Y., et al., 2018. Comparative effects of nano and bulk-Fe3O4 on the growth of cucumber (Cucumis sativus). Ecotoxicol. Environ. Saf. 165, 547–554.

Li, J., Hu, J., Ma, C., Wang, Y., Wu, C., Huang, J., Xing, B., 2016. Uptake, translocation and physiological effects of magnetic iron oxide (γ-Fe2O3) nanoparticles in corn (Zea mays L.). Chemosphere 159, 326–334.

Li, J., Hu, J., Xiao, L., Wang, Y., Wang, X., 2018. Interaction mechanisms between α-Fe$_2$O$_3$, γ-Fe$_2$O$_3$ and Fe$_3$O$_4$ nanoparticles and Citrus maxima seedlings. Sci. Total Environ. 625, 677–685.

Lichtenthaler, H.K., Wellburn, A.R., 1983. Determinations of total carotenoids and chlorophylls a and b of leaf extracts in different solvents. Biochem. Soc. Trans. 11 (5), 591–592.

Liu, R., Lal, R., 2015. Potentials of engineered nanoparticles as fertilizers for increasing agronomic productions. Sci. Total Environ. 514, 131–139.

Ma, X., Gurung, A., Deng, Y., 2013. Phytotoxicity and uptake of nanoscale zero-valent iron (nZVI) by two plant species. Sci. Total Environ. 443, 844–849.

Marusenko, Y., Shipp, J., Hamilton, G.A., Morgan, J.L., Keebaugh, M., Hill, H., et al., 2013. Bioavailability of nanoparticulate hematite to Arabidopsis thaliana. Environ. Pollut. 174, 150–156.

Moore, M.N., 2006. Do nanoparticles present ecotoxicological risks for the health of the aquatic environment? Environ. Int. 32, 967–976.

Morales-Díaz, A.B., Ortega-Ortíz, H., Juárez-Maldonado, A., Cadenas-Pliego, G., González-Morales, S., Benavides-Mendoza, A., 2017. Application of nanoelements in plant nutrition and its impact in ecosystems. Adv. Nat. Sci. Nanosci. Nanotechnol 8 (1), 013001.

Mushtaq, Y.K., 2011. Effect of nanoscale Fe3O4, TiO2 and carbon particles on cucumber seed germination. J. Environ. Sci. Health A 46 (14), 1732–1735.

Nikalje, A.P., 2015. Nanotechnology and its applications in medicine. Med. Chem. 5 (2), 081–089.

Parisi, C., Vigani, M., Rodríguez-Cerezo, E., 2015. Agricultural nanotechnologies: what are the current possibilities. Nano Today 10 (2), 124–127.

Pérez-de-Luque, A., 2017. Interaction of nanomaterials with plants: what do we need for

real applications in agriculture? Front. Env. Sci. 5, 12.

Prasad, R., Kumar, V., Prasad, K.S., 2014. Nanotechnology in sustainable agriculture: present concerns and future aspects. Afr. J. Biotechnol. 13 (6), 705–713.

Rai, P.K., Kumar, V., Lee, S., Raza, N., Kim, K.H., Ok, Y.S., Tsang, D.C., 2018. Nanoparticle-plant interaction: implications in energy, environment, and agriculture. Environ. Int. 119, 1–19.

Rico, C.M., Majumdar, S., Duarte-Gardea, M., Peralta-Videa, J.R., Gardea-Torresdey, J.L., 2011. Interaction of nanoparticles with edible plants and their possible implications in the food chain. J. Agric. Food Chem. 59, 3485–3498.

Rout, G.R., Sahoo, S., 2015. Role of iron in plant growth and metabolism. Rev. Agric. Sci. 3, 1–24.

Rui, M., Ma, C., Hao, Y., Guo, J., Rui, Y., Tang, X., et al., 2016. Iron oxide nanoparticles as a potential iron fertilizer for peanut (Arachis hypogaea). Front. Plant Sci. 7, 815.

Samaranayake, P., Peiris, B.D., Dssanayake, S., 2012. Effect of excessive ferrous (Fe^{2+}) on growth and iron content in rice (Oryza sativa). Int. J. Agric. Biol. 14 (2).

Surendar, K.K., Devi, D.D., Ravi, I., Jeyakumar, P., Velayudham, K., 2013. Water stress affects plant relative water content, soluble protein, total chlorophyll content and yield of ratoon banana. Int. J. Hortic. 3, 96–103.

Teixeira, J., Pereira, S., Cánovas, F., Salema, R., 2005. Glutamine synthetase of potato (Solanum tuberosum L. cv. Desiree) plants: cell-and organ-specific expression and differential developmental regulation reveal specific roles in nitrogen assimilation and mobilization. J. Exp. Bot. 56 (412), 663–671.

Tombuloglu, H., Tombuloglu, G., Slimani, Y., Ercan, I., Sozeri, H., Baykal, A., 2018. Impact of manganese ferrite (MnFe2O4) nanoparticles on growth and magnetic character of barley (Hordeum vulgare L.). Environ. Pollut. 243, 872–881.

Tombuloglu, G., Tombuloglu, H., Sakcali, M.S., Unver, T., 2015. High-throughput transcriptome analysis of barley (Hordeum vulgare) exposed to excessive boron. Gene 557 (1), 71–81.

Tombuloglu, H., Kekec, G., Sakcali, M.S., Unver, T., 2013. Transcriptome-wide identification of R2R3-MYB transcription factors in barley with their boron responsive expression analysis. Mol. Genet. Genom. 288 (3–4), 141–155.

United States Environmental Protection Agency, 1996. Ecological Effects Test Guidelines: Seed Germination/root Elongation Toxicity Test. Prevention, Pesticides and Toxic Substances (7101), Washington, DC.

Wang, H., Kou, X., Pei, Z., Xiao, J.Q., Shan, X., Xing, B., 2011. Physiological effects of magnetite (Fe3O4) nanoparticles on perennial ryegrass (Lolium perenne L.) and pumpkin (Cucurbita mixta) plants. Nanotoxicology 5 (1), 30–42.

Wang, P., Lombi, E., Zhao, F.J., Kopittke, P.M., 2016. Nanotechnology: a new opportunity in plant sciences. Trends Plant Sci. 21 (8), 699–712.

White, P.J., Broadley, M.R., 2009. Biofortification of crops with seven mineral elements often lacking in human diets–iron, zinc, copper, calcium, selenium and iodine. New Phytol. 182 (1), 49–84.

Zhai, G., Walters, K.S., Peate, D.W., Alvarez, P.J., Schnoor, J.L., 2014. Transport of gold nanoparticles through plasmodesmata and precipitation of gold ions in woody poplar. Environ. Sci. Technol. Lett. 1 (2), 146–151.

Zhu, H., Han, J., Xiao, J.Q., Jin, Y., 2008. Uptake, translocation, and accumulation of manufactured iron oxide nanoparticles by pumpkin plants. J. Environ. Monit. 10 (6), 713–717.

Zuo, Y., Zhang, F., 2011. Soil and crop management strategies to prevent iron deficiency in crops. Plant Soil 339 (1–2), 83–95.